JOURNAL OF NATURAL PRODUCTS

Article

pubs.acs.org/jnp

Cytotoxic 14-Membered Macrolides from a Mangrove-Derived Endophytic Fungus, *Pestalotiopsis microspora*

Shuai Liu,[†] Haofu Dai,[‡] Gamall Makhloufi,[§] Christian Heering,[§] Christoph Janiak,[§] Rudolf Hartmann,[⊥] Attila Mándi,[#] Tibor Kurtán,[#] Werner E. G. Müller,[∥] Matthias U. Kassack,[○] Wenhan Lin,[¶] Zhen Liu,*[,†] and Peter Proksch*[,†]

[†]Institute of Pharmaceutical Biology and Biotechnology, [§]Institute of Inorganic and Structural Chemistry, and [○]Institute of Pharmaceutical and Medicinal Chemistry, Heinrich-Heine-Universität Düsseldorf, Universitätsstrasse 1, 40225 Düsseldorf, Germany

[‡]Key Laboratory of Biology and Genetic Resources of Tropical Crops, Ministry of Agriculture, Institute of Tropical Bioscience and Biotechnology, Chinese Academy of Tropical Agricultural Sciences, Haikou 571101, China

[⊥]Institute of Complex Systems: Strukturbiochemie, Forschungszentrum Juelich, Wilhelm-Johnen-Straße, 52428 Juelich, Germany

[#]Department of Organic Chemistry, University of Debrecen, P.O. Box 400, H-4002 Debrecen, Hungary

[∥]Institute of Physiological Chemistry, Universitätsmedizin der Johannes Gutenberg-Universität Mainz, Duesbergweg 6, 55128 Mainz, Germany

[¶]State Key Laboratory of Natural and Biomimetic Drugs, Peking University, Beijing 100191, China

Supporting Information

ABSTRACT: Seven new 14-membered macrolides, pestalotioprolides C (**2**), D−H (**4**−**8**), and 7-*O*-methylnigrosporolide (**3**), together with four known analogues, pestalotioprolide B (**1**), seiricuprolide (**9**), nigrosporolide (**10**), and 4,7-dihydroxy-13-tetradeca-2,5,8-trienolide (**11**), were isolated from the mangrove-derived endophytic fungus *Pestalotiopsis microspora*. Their structures were elucidated by analysis of NMR and MS data and by comparison with literature data. Single-crystal X-ray diffraction analysis was used to confirm the absolute configurations of **1**, **2**, and **10**, while Mosher's method and the TDDFT-ECD approach were applied to determine the absolute configurations of **5** and **6**. Compounds **3**−**6** showed significant cytotoxicity against the murine lymphoma cell line L5178Y with IC_{50} values of 0.7, 5.6, 3.4, and 3.9 μM, respectively, while compound **5** showed potent activity against the human ovarian cancer cell line A2780 with an IC_{50} value of 1.2 μM. Structure−activity relationships are discussed. Coculture of *P. microspora* with *Streptomyces lividans* caused a roughly 10-fold enhanced accumulation of compounds **5** and **6** compared to axenic fungal control.

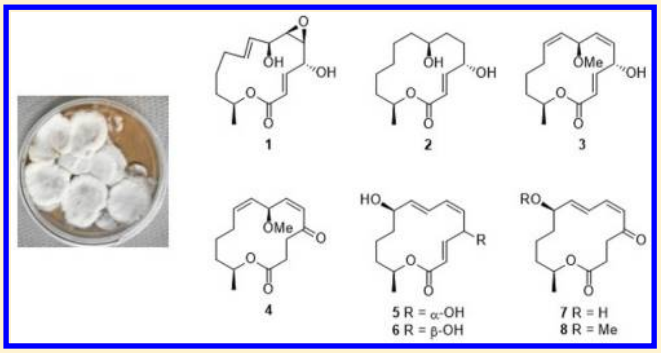

Since the discovery of the well-known antibiotic erythromycin in 1952, naturally occurring macrolides have attracted considerable attention due to their diverse structures and promising biological properties such as antibacterial, antitumoral, and anti-inflammatory effects.[1] They are biogenetically derived through the polyketide synthase pathways in bacteria and in fungi.[2] Previously, several 14-membered macrolides exhibiting different bioactivities were isolated from fungi, including the phytotoxic compound seiricurprolide obtained from *Seiridium cupressi*[3] and the mycotoxin zearalenone, a resorcinonic 14-membered macrolide, which is derived from fungi of the genus *Fusarium* and possesses estrogenic activity in pigs, cattle, and sheep.[4] Further examples include aspergillides A−C, isolated from the marine-derived fungus *Aspergillus ostianus*, which exhibit cytotoxicity against L1210 mouse lymphocytic leukemia cells.[5] In the course of our ongoing studies on new bioactive natural products from endophytic fungi,[6−9] *Pestalotiopsis microspora* was isolated from fresh fruits of the mangrove plant *Drepanocarpus lunatus* (Fabaceae) collected in Cameroon, which resulted in the isolation of 11 14-membered macrolides (**1**−**11**) including seven new compounds, pestalotioprolides C (**2**) and D−H (**4**−**8**) and 7-*O*-methylnigrosporolide (**3**). On the basis of our previous studies on cocultivation of fungi with bacteria,[10,11] coculture experiments of *P. microspora* with *Streptomyces lividans* were carried out. Compared to the axenically grown fungus, cocultivation of *P. microspora* with *S. lividans* resulted in a strong increase in the production of **5** and **6**. In this paper we report the isolation, structure elucidation, and cytotoxic activities of the macrolides, as well as the cocultivation results.

Received: May 24, 2016
Published: August 24, 2016

DOI: 10.1021/acs.jnatprod.6b00473
J. Nat. Prod. 2016, 79, 2332−2340

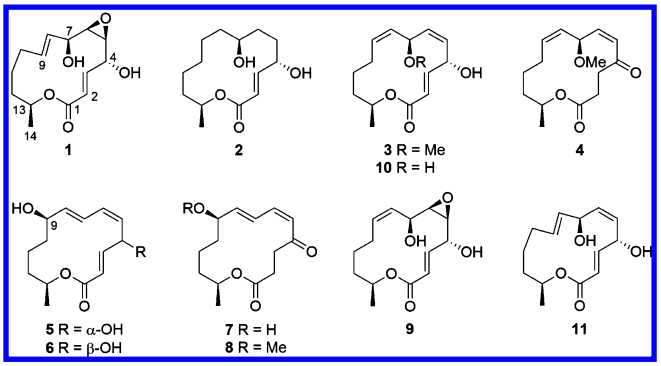

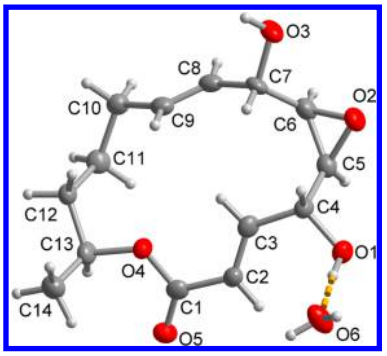

Figure 1. Molecular structure of **1** from single-crystal X-ray diffractometry.

RESULTS AND DISCUSSION

Compound **1** was obtained as colorless crystals. Its molecular formula $C_{14}H_{20}O_5$ was established by HRESIMS. The ^{13}C and ^{1}H NMR data of **1** (Table 1) were similar to those of seiricuprolide (**9**).[3] Detailed analysis of the 2D NMR spectra of **1** revealed that it was the known compound pestalotioprolide B, which was previously isolated as a diacetate derivative by Rukachaisirikul et al. because it was difficult to separate it from seiricuprolide (**9**).[12] However, the use of a chiral-phase HPLC column in our study overcame this problem. The absolute configuration of **1** was determined as 4*R*, 5*S*, 6*R*, 7*S*, and 13*S* by X-ray single-crystal diffraction (Figure 1).

The molecular formula of pestalotioprolide C (**2**) was determined as $C_{14}H_{24}O_4$ by HRESIMS, lacking two degrees of unsaturation compared to **1**. As expected, the NMR spectra of **2** showed one ester carbonyl carbon at δ_C 167.8 (C-1), signals of an α,β-unsaturated double bond at δ_C 152.0 (C-3), 121.8 (C-2) and at δ_H 6.96 (dd, H-3), 6.00 (dd, H-2), three oxygenated methine groups at δ_C 73.7 (C-13), 70.7 (C-4), and 70.7 (C-7) and at δ_H 5.01 (m, H-13), 4.48 (m, H-4), and 3.57 (m, H-7), and one methyl group at δ_C 21.0 (C-14) and δ_H 1.27 (d, H_3-14). However, the signals for the C-5/C-6 epoxy unit and the C-8/C-9 double bond of **1** were missing. Instead, seven

Table 1. ^{1}H and ^{13}C NMR Data for Compounds 1−4

	1[a]		2[b]		3[c]		4[b]	
position	δ_C, type	δ_H (J in Hz)	δ_C, type	δ_H (J in Hz)	δ_C, type	δ_H (J in Hz)	δ_C, type	δ_H (J in Hz)
1	166.1, C		167.8, C		168.4, C		174.7, C	
2	120.9, CH	5.99, dd (15.5, 2.0)	121.8, CH	6.00, dd (15.7, 1.8)	121.5, CH	6.09, dd (15.5, 1.3)	30.0, CH_2	2.80, ddd (15.0, 10.9, 2.8)
								2.41, ddd (15.0, 6.7, 2.9)
3	148.2, CH	7.11, dd (15.5, 4.0)	152.0, CH	6.96, dd (15.7, 4.2)	150.0, CH	6.93, dd (15.5, 6.9)	41.0, CH_2	2.96, ddd (17.8, 10.9, 2.9)
								2.74, ddd (17.8, 6.7, 2.8)
4	71.4, CH	4.32, m	70.7, CH	4.48, m	69.7, CH	5.17, m	201.5, C	
5	61.8, CH	2.92, dd (5.6, 4.6)	32.6, CH_2	1.92, m	136.3, CH	5.65, dd (11.4, 4.4)	127.4, CH	6.32, dd (11.5, 0.9)
				1.74, m				
6	59.3, CH	2.94, dd (8.9, 4.6)	30.4, CH_2	1.56, m	130.4, CH	5.27, ddd (11.4, 10.1, 2.3)	145.5, CH	5.90, dd (11.5, 9.6)
				1.34, m				
7	71.7, CH	3.94, ddd (8.9, 7.7, 3.9)	70.7, CH	3.57, m	73.4, CH	4.70, dd (10.1, 9.5)	73.0, CH	5.79, m
8	130.9, CH	5.55, dd (15.6, 7.7)	36.2, CH_2	1.42, m	128.6, CH	5.14, m	129.8, CH	5.23, m
9	135.2, CH	5.96, m	25.0, CH_2	1.42, m	135.2, CH	5.49, ddd (11.0, 11.0, 3.4)	135.0, CH	5.67, m
				1.25, m				
10	33.7, CH_2	2.12, m	29.6, CH_2	1.46, m	30.8, CH_2	2.55, m	30.0, CH_2	2.12, m
		2.01, m		1.24, m		1.98, m		1.85, m
11	25.4, CH_2	1.86, m	26.2, CH_2	1.47, m	26.9, CH_2	1.75, m	28.3, CH_2	1.31, m
		1.13, m		1.18, m		1.09, m		0.92, m
12	35.1, CH_2	1.80, m	35.8, CH_2	1.74, m	35.6, CH_2	1.90, m	37.4, CH_2	1.64, m
		1.56, m		1.51, m		1.47, m		1.54, m
13	72.3, CH	4.66, m	73.7, CH	5.01, m	74.3, CH	4.96, m	73.1, CH	4.90, m
14	20.3, CH_3	1.22, d (6.2)	21.0, CH_3	1.27, d (6.4)	20.7, CH_3	1.28, d (6.2)	20.4, CH_3	1.24, d (6.4)
4-OH		4.99, d (4.4)						
7-OH		4.17, d (3.9)						
7-OMe					55.4, CH_3	3.28, s	56.1, CH_3	3.30, s

[a]Recorded at 600 MHz (^{1}H) and 150 MHz (^{13}C) in CD_3COCD_3. [b]Recorded at 600 MHz (^{1}H) and 150 MHz (^{13}C) in CD_3OD. [c]Recorded at 700 MHz (^{1}H) and 175 MHz (^{13}C) in CD_3OD.

DOI: 10.1021/acs.jnatprod.6b00473
J. Nat. Prod. 2016, 79, 2332−2340

aliphatic methylene groups were observed in **2** at δ_C 36.2 (C-8), 35.8 (C-12), 32.6 (C-5), 30.4 (C-6), 29.6 (C-10), 26.2 (C-11), and 25.0 (C-9), suggesting the replacement of the C-5/C-6 epoxy ring and the C-8/C-9 double bond by four aliphatic methylene groups in **2**. This was further confirmed by the COSY correlations between H-4/H_2-5, H_2-5/H_2-6, H_2-6/H-7, H-7/H_2-8, and H_2-8/H_2-9 and by the HMBC correlations from H-3 to C-5, from H-4 to C-5 and C-6, and from H-7 to C-5 and C-9. Thus, pestalotioprolide C (**2**) was identified as shown, and its absolute configuration was determined as 4*S*, 7*S*, 13*S* by X-ray single-crystal diffraction analysis (Figure 2).

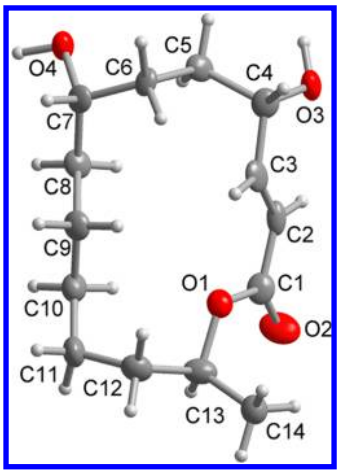

Figure 2. Molecular structure of **2** from single-crystal X-ray diffractometry.

Compound **3** was isolated as a colorless oil. Its molecular formula was established as $C_{15}H_{22}O_4$ by HRESIMS, containing an additional methyl substituent in comparison with nigrosporolide (**10**).[13] The NMR spectra of **3** were closely related to those of **10** except for the appearance of an additional methoxy group at δ_C 55.4 and δ_H 3.28. The location of this methoxy group at C-7 in **3** was confirmed by the HMBC correlation from its protons to C-7 (δ_C 73.4) and in turn from H-7 (δ_H 4.70, dd) to the carbon of the methoxy group. Thus, compound **3** was elucidated as 7-*O*-methylnigrosporolide. The relative configuration of nigrosporolide (**10**) was not disclosed in the previous report by Harwooda et al.[13] However, in our present study, we crystallized **10** and, by use of X-ray analysis, determined its absolute configuration as 4*S*, 7*S*, 13*S* (Figure 3). Considering the similarity of coupling constants and NOE correlations in **3** and **10**, as well as their close biogenetic relationship, the absolute configuration of **3** is proposed to be identical to **10**.

Pestalotioprolide D (**4**) shared the same molecular formula as **3** as deduced by HRESIMS. Comparison of the ^1H and ^{13}C NMR data of **4** with those of **3** revealed the presence of one additional ketone carbonyl (δ_C 201.5, C-4) and two additional methylene groups (δ_C 41.0, δ_H 2.96 and 2.74, CH_2-3; δ_C 30.0, δ_H 2.80 and 2.41, CH_2-2), as well as the disappearance of one double bond and one oxygenated methine in **4** compared to **3**. In the HMBC spectrum of **4**, both H-2ab and H-3ab exhibited correlations to C-1 (δ_C 174.7) and C-4, while H-5 (δ_H 6.32) showed a correlation to C-4, indicating the CO(1)−CH_2(2)−CH_2(3)−CO(4) fragment. The remaining substructure of **4** was found to be identical to that of **3**, as confirmed by detailed interpretation of the 2D NMR data. The similar *J* values and ROESY relationships between **3** and **4** suggested that both

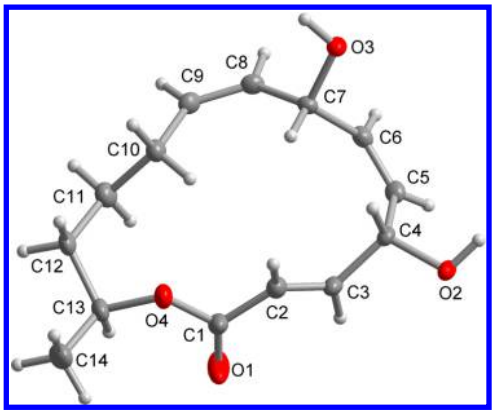

Figure 3. Molecular structure of **10** from single-crystal X-ray diffractometry.

compounds had the same configuration at the stereogenic centers C-7 and C-13 as 7*S* and 13*S*.

On the basis of the HRESIMS data, the molecular formula of pestalotioprolide E (**5**) was established to be the same as that of the known nigrosporolide (**10**).[13] Six olefinic methine protons at δ_H 7.27 (dd, H-3), 6.44 (dd, H-7), 6.14 (dd, H-6), 6.06 (dd, H-2), 5.71 (dd, H-5), and 5.51 (dd, H-8) and three oxygenated methine protons at δ_H 5.15 (m, H-13), 4.90 (ddd, H-4), and 4.04 (m, H-7) were observed in the ^1H NMR spectrum of **5** (Table 2). However, the observed COSY correlations between H-4/H-5, H-5/H-6, H-6/H-7, H-7/H-8, and H-8/H-9 indicated the conjugated double bonds of **5** to be located at C-5/C-6 and C-7/C-8, whereas a hydroxy group was present at C-9. Detailed analysis of 1D and 2D NMR spectra of **5** revealed the remaining structure of **5** to be identical to that of **10**. The configurations of the three double bonds in **5** were elucidated as 2*E*, 5*Z*, and 7*E*, respectively, on the basis of the coupling constants ($^2J_{2,3}$ = 15.8 Hz, $^2J_{5,6}$ = 11.3 Hz, $^2J_{7,8}$ = 15.6 Hz). The configuration of C-13 in **5** was assumed to be the same as that of the other pestalotioprolides due to biogenetic considerations. Mosher's method was applied to determine the absolute configuration of C-4 and C-9. Treatment of **5** with 2 equiv of (*R*)- or (*S*)-MTPACl yielded ester **5a** or **5b**, respectively (Figure 4). However, a double-bond rearrangement occurred from C-2 to C-3 during the acylation reaction, which was previously also described by Jiao et al.[14] This rearrangement prevented assignment of the C-4 absolute configuration. Analysis of the chemical shift differences $\Delta\delta^{SR}$ ($\delta_S - \delta_R$) between **5a** and **5b** indicated the 9*R* configuration.

Pestalotioprolide F (**6**) possessed the same molecular formula as **5** as determined by HRESIMS data. Detailed analysis of the COSY and HMBC spectra indicated that both compounds also had the same planar structure. The coupling constants ($^2J_{2,3}$ = 15.7 Hz, $^2J_{5,6}$ = 11.7 Hz, $^2J_{7,8}$ = 15.4 Hz) were in accord with 2*E*, 5*Z*, and 7*E* double-bond configurations. However, H-4 shifted to δ_H 5.08 in **6**, compared to the corresponding chemical shift for H-4 at δ_H 4.90 in **5**. Meanwhile, the coupling constants ($^2J_{3,4}$ = 6.2 Hz, $^2J_{4,5}$ = 3.8 Hz) in **6** were different from those in **5** ($^2J_{3,4}$ = 3.2 Hz, $^2J_{4,5}$ = 7.0 Hz), suggesting **6** to be the 4-epimer of **5**. In the ROESY spectrum, correlations between H-3/H-7, H-7/H-9, H-5/H-6, and H-6/H-8 were observed in both **5** and **6**. However, H-4 showed an NOE correlation to H-2 but not to H-7 in compound **5**, in contrast to the NOE correlation from H-4 to H-7 but not to H-2 in compound **6** (Figure 5). Because the absolute configuration of C-9 in **5** was determined to be *R* by

DOI: 10.1021/acs.jnatprod.6b00473
J. Nat. Prod. 2016, 79, 2332−2340

Table 2. ^{1}H and ^{13}C NMR Data for Compounds 5−8

	5[a]		6[a]		7[b]		8[a]	
position	δ_C, type	δ_H (J in Hz)	δ_C, type	δ_H (J in Hz)	δ_C, type	δ_H (J in Hz)	δ_C, type	δ_H (J in Hz)
1	167.7, C		168.3, C		171.7, C		173.0, C	
2	120.4, CH	6.06, dd (15.8, 2.3)	121.6, CH	6.03, dd (15.7, 1.2)	30.4, CH_2	2.67, m	30.5, CH_2	2.68, m
						2.51, m		2.53, m
3	154.3, CH	7.27, dd (15.8, 3.2)	151.2, CH	7.11, dd (15.7, 6.2)	39.0, CH_2	2.78, m	38.7, CH_2	2.76, m
						2.71, m		2.69,m
4	68.9, CH	4.90, ddd (7.0, 3.2, 2.3)	70.4, CH	5.08, ddd (6.2, 3.8, 1.2)	202.5, C		204.5, C	
5	130.6, CH	5.71, dd (11.3, 7.0)	133.9, CH	5.55, dd (11.7, 3.8)	129.4, CH	6.15, d (11.5)	129.4, CH	6.19, d (11.6)
6	132.0, CH	6.14, dd (11.3, 10.7)	129.3, CH	6.02, dd (11.7, 10.9)	136.8, CH	6.45, dd (11.5, 10.7)	137.1, CH	6.50, dd (11.6, 10.7)
7	128.6, CH	6.44, dd (15.6, 10.7)	129.0, CH	6.40, dd (15.4, 10.9)	126.5, CH	6.55, dd (15.8, 10.7)	129.5, CH	6.70, dd (15.9, 10.7)
8	139.2, CH	5.51, dd (15.6, 6.8)	138.3, CH	5.47, dd (15.4, 7.6)	143.6, CH	5.77, dd (15.8, 7.4)	141.3, CH	5.70, dd (15.9, 7.8)
9	72.4, CH	4.04, m	72.7, CH	4.04, m	72.2, CH	4.17, m	82.7, CH	3.75, m
10	35.7, CH_2	1.55, m	36.0, CH_2	1.51, m	35.9, CH_2	1.71, m	33.2, CH_2	1.73, m
						1.36, m		1.36, m
11	18.5, CH_2	1.48, m	21.5, CH_2	1.42, m	19.4, CH_2	1.38, m	19.4, CH_2	1.36, m
		1.36, m		1.01, m		1.19, m		1.18, m
12	35.1, CH_2	1.71, m	37.1, CH_2	1.65, m	34.6, CH_2	1.66, m	34.4, CH_2	1.69, m
		1.52, m		1.58, m		1.37, m		1.35, m
13	71.6, CH	5.15, m	72.7, CH	4.90, m	70.9, CH	4.95, m	72.0, CH	4.99, m
14	19.0, CH_3	1.28, d (6.5)	21.0, CH_3	1.29, d (6.3)	19.3, CH_3	1.12, d (6.4)	18.9, CH_3	1.15, d (6.5)
9-OH						3.97, d (3.5)		
9-OMe							56.6, CH_3	3.29, s

[a]Recorded at 600 MHz (^{1}H) and 150 MHz (^{13}C) in CD_3OD. [b]Recorded at 600 MHz (^{1}H) and 150 MHz (^{13}C) in CD_3COCD_3.

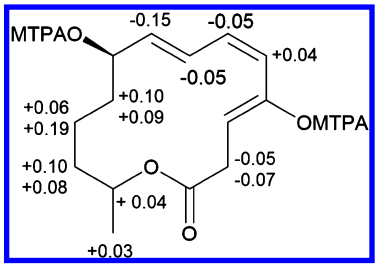

Figure 4. $\Delta\delta^{SR}$ ($\delta_S - \delta_R$) values of (*S*)-MTPA ester **5a** and (*R*)-MTPA ester **5b**.

Mosher's method, the above findings indicated the 4*S* configuration for **5** and the 4*R* configuration for **6**, respectively.

The TDDFT-ECD approach was pursued to confirm the above assignment. A conjugated diene and an α,β-unsaturated lactone chromophore can be found in **5**, which gave rise to a strong positive Cotton effect (CE) at 235 nm (Figure 6). DFT reoptimization of the initial 217 MMFF conformers of (4*S*,9*R*,13*S*)-**5** resulted in 18 and 15 conformers at the B3LYP/6-31G(d) in vacuo and B97D/TZVP PCM/MeCN levels, respectively. The ECD spectra computed for the above conformers reproduced the intense positive CE at 234 nm and the negative one below 195 nm, while the weak low-energy positive n−π* shoulder could not be reproduced well. On the basis of the good overall agreement of the π−π* transitions, the absolute configuration of **5** could be assigned as (4*S*, 9*R*, 13*S*).

DFT reoptimization of the initial 274 MMFF conformers of (4*R*,9*R*,13*S*)-**6** resulted in 15, 20, and 20 conformers at the B3LYP/6-31G(d) in vacuo, B97D/TZVP PCM/MeCN, and CAM-B3LYP/TZVP PCM/MeCN levels, respectively. All the ECD calculations performed on all sets of conformers

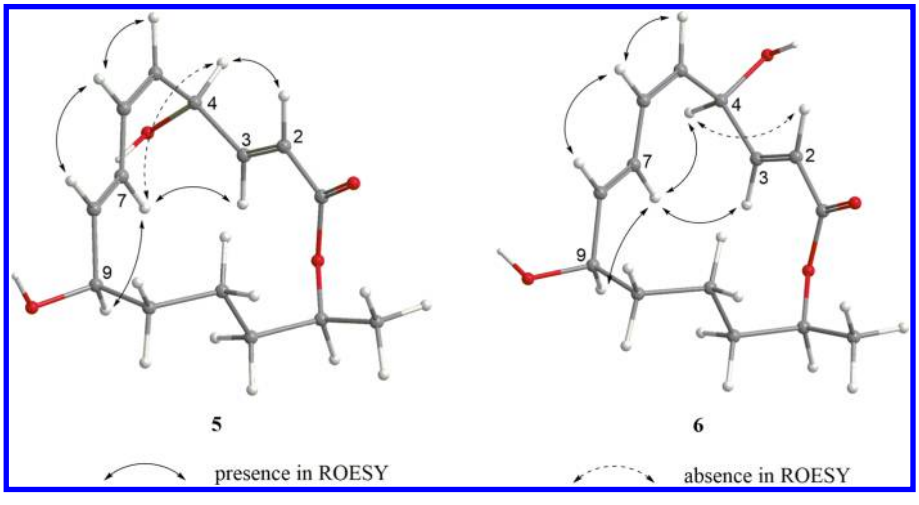

Figure 5. Key NOE correlations in compounds **5** and **6**.

DOI: 10.1021/acs.jnatprod.6b00473
J. Nat. Prod. 2016, 79, 2332−2340

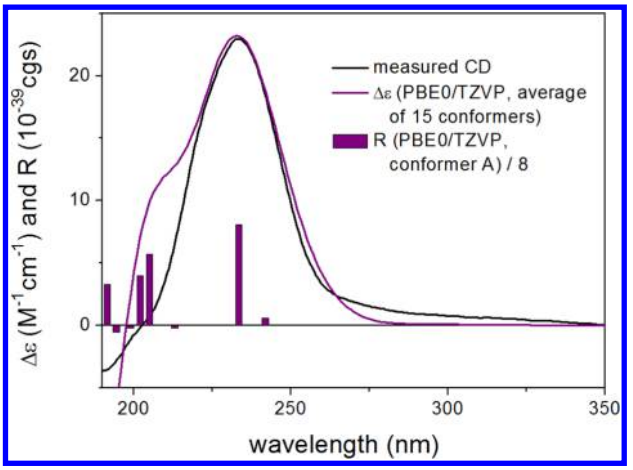

Figure 6. Experimental ECD spectrum of **5** in MeCN compared with the Boltzmann-weighted PBE0/TZVP PCM/MeCN ECD spectrum of (4*S*,9*R*,13*S*)-**5** computed for the B97D/TZVP PCM/MeCN conformers. Bars represent the rotational strength of the lowest energy conformer.

reproduced the strong $\pi-\pi^*$ transitions at 233 and 207 nm, while the weak negative transition at 288 nm could be reproduced only by the in vacuo calculations performed on the B3LYP/6-31G(d)-reoptimized conformers and the weak positive $n-\pi^*$ transition at 351 nm could not be reproduced at any applied level (Figure 7). The good agreement of the high-energy ECD transitions allowed the safe elucidation of the absolute configuration of **6** as (4*R*, 9*R*, 13*S*).

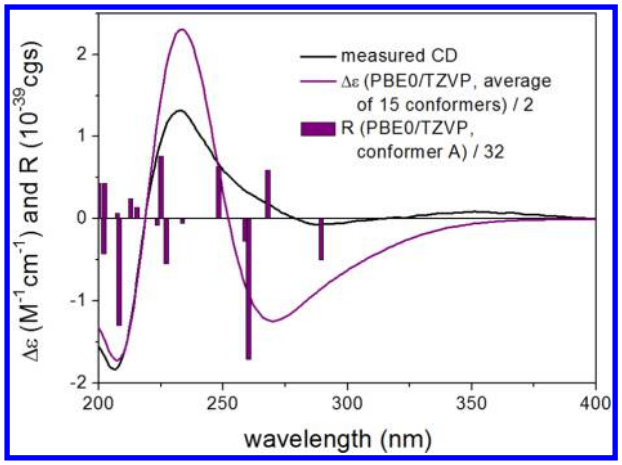

Figure 7. Experimental ECD spectrum of **6** in MeCN compared with the Boltzmann-weighted PBE0/TZVP ECD spectrum of (4*R*,9*R*,13*S*)-**6** computed for the B3LYP/6-31G(d) in vacuo conformers. Bars represent the rotational strength of the lowest energy conformer.

Pestalotioprolide G (**7**) was obtained as a colorless oil, possessing the molecular formula $C_{14}H_{20}O_4$ as determined from the HRESIMS spectrum. Comparison of the ^{1}H and ^{13}C NMR data revealed that the segment from C-1 to C-4 of **7** was the same as that of **4**, whereas the substructure from C-5 to C-14 was compatible with that of **5** and **6**, which was further confirmed by analysis of 2D NMR spectra. The configurations of C-7 and C-13 in **7** were assumed to be the same as those of **5** and **6** due to their similar NMR data and the biogenetic relationship of the respective compounds.

Compound **8** was elucidated as the C-9 *O*-methyl derivative of **7**, as evident from the appearance of an additional methoxy group (δ_C 56.6, δ_H 3.29) in **8** and the HMBC correlation from its protons to the obvious deshielded C-9 (δ_C 82.7). The similarity of the NMR data including NOE correlations between **7** and **8** suggested the same configurations for both compounds.

The remaining three known compounds were identified as seiricuprolide (**9**),[3] nigrosporolide (**10**),[13] and 4,7-dihydroxy-13-tetradeca-2,5,8-trienolide (**11**),[15,16] respectively. All substances (**1**–**11**) were tested for their cytotoxicity against the L5178Y mouse lymphoma cell line using the MTT assay (Table 3). Among them, **3** exhibited potent activity with an IC_{50} value of 0.7 μM, which was even stronger than that of the positive control kahalalide F (IC_{50} 4.3 μM). Compounds **4**, **5**, **6**, and **8** were less active, with IC_{50} values of 5.6, 3.4, 3.9, and 11 μM, respectively, whereas the other macrolides showed weak or no activity (IC_{50} > 20 μM). On the basis of these bioassay data, some preliminary structure–activity relationships can be concluded. The epoxy group at C-5/C-6 (**1** vs **11**; **9** vs **10**) apparently resulted in total loss of cytotoxicity. The rearrangement of the double bond from C-2/C-3 to the C-3 ketone (**3** vs **4**; **5** and **6** vs **7**) decreased the cytotoxicity. The 8*Z* or 8*E* configuration (**9** vs **1**; **10** vs **11**) and 4*R* or 4*S* configuration (**6** vs **5**) had little influence on the cytotoxicity. Moreover, the hydroxy group replaced by the methoxy substituent at C-7 (**10** vs **3**) or C-9 (**7** vs **8**) led to a strong increase of cytotoxicity. In addition to the experiments with the murine lymphoma cell line, cytotoxicity of all isolated macrolides was also evaluated against the human ovarian cancer cell line A2780 (Table 3). Only compound **5** showed significant activity, with an IC_{50} value of 1.2 μM, which was comparable to that of the positive control cisplatin (IC_{50} 1.2 μM). Compound **6** (IC_{50} 12 μM) was less active, and the others (IC_{50} > 20 μM) exhibited weak or no activity. These differences in activity may reflect species specific (murine vs human) or cell line specific (blood cancer vs solid cancer) differences in susceptibility against the studied compounds.

Coculture experiments of *P. microspora* employing different inoculation volumes of *S. lividans* were carried out (Figure 8). Compared with the axenic fungal control, strong enhancements of compounds **5** (9.0-fold increase) and **6** (10.4-fold increase) were found in the coculture with 0.2 g of *S. lividans* per flask (Table 4). However, for Δ^8 isomers **10** and **11**, only a small increase (1.3-fold) was observed. Meanwhile, some unidentified macrolides were also detected in the coculture extracts as suggested by comparison of their UV patterns and MS data with those of the isolated macrolides. The structures of these compounds were not elucidated due to their small amounts.

Table 3. Cytotoxicity (IC_{50}, μM) of 1–11 against the L5178Y and A2780 Cell Lines

	1	2	3	4	5	6	7	8	9	10	11
L5178Y[a]	–[c]	39	0.7	5.6	3.4	3.9	–	11	–	21	21
A2780[b]	–	–	28	–	1.2	12	36	–	–	43	–

[a]Kahalalide F (IC_{50} 4.3 μM) as positive control. [b]Cisplatin (IC_{50} 1.2 μM) as positive control. [c]IC_{50} > 50 μM.

DOI: 10.1021/acs.jnatprod.6b00473
J. Nat. Prod. 2016, 79, 2332–2340

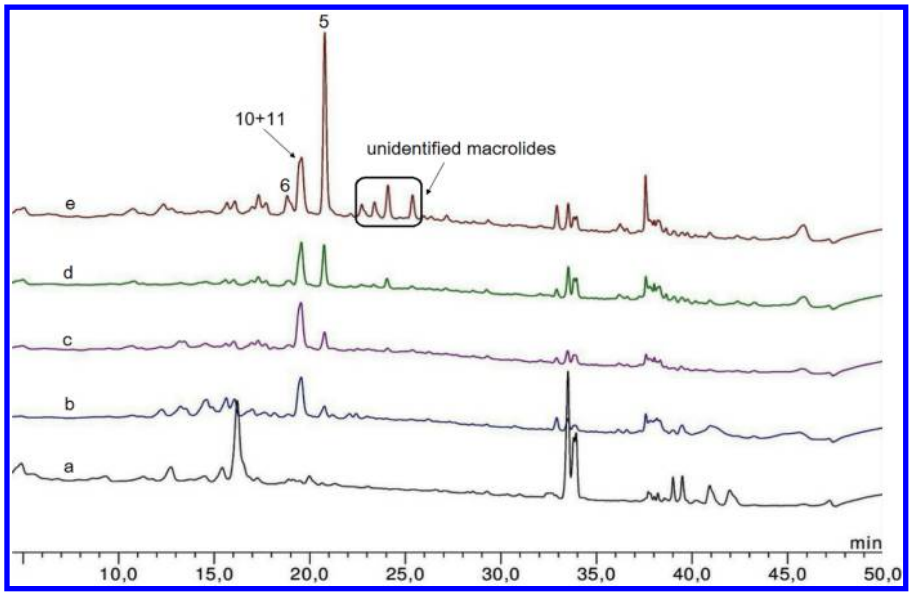

Figure 8. HPLC analysis of the EtOAc extract from cocultivation experiments detected at UV 235 nm: (a) axenic control of *S. lividans*, (b) axenic control of *P. microspora*, (c) coculture of *P. microspora* with *S. lividans* (0.05 g/flask), (d) coculture of *P. microspora* with *S. lividans* (0.1 g/flask), (e) coculture of *P. microspora* with *S. lividans* (0.2 g/flask).

Table 4. Yield of Macrolides per Flask during Coculture of *P. microspora* with Different Inoculation Volumes of *S. lividans* (n = 3) vs Axenic Controls of *P. microspora* (n = 3)[a]

	5	6	10 + 11
control of *P. microspora*	0.52 ± 0.11	0.10[b]	5.35 ± 1.09
coculture of *P. microspora* with *S. lividans* (0.05 g/flask)	0.53 ± 0.05	not detected	5.21 ± 0.49
coculture of *P. microspora* with *S. lividans* (0.1 g/flask)	1.17 ± 0.14	0.44 ± 0.05	4.32 ± 0.52
coculture of *P. microspora* with *S. lividans* (0.2 g/flask)	4.70 ± 0.97	1.04 ± 0.22	6.71 ± 1.39
coculture of *P. microspora* with *S. lividans* (0.2 g/flask) vs control of *P. microspora* (fold)	9.0	10.4	1.3

[a]Amounts of compounds are reported in mg/1 L flask. [b]Calculation was performed using the actual isolated amount because it could not be detected by HPLC.

These experiments suggested that the production of fungal secondary metabolites can be induced by cocultivation with *S. lividans*, and higher inoculation volumes of bacteria seemed to be more effective in provoking this induction.

In summary, chemical examination of the endophytic fungus *P. microspora* resulted in the isolation of 11 14-membered macrolides, including seven new compounds, pestalotioprolides C (**2**) and D−H (**4**−**8**) and 7-*O*-methylnigrosporolide (**3**). All compounds are suggested to have the 13*S* configuration, as demonstrated by X-ray crystallography for compounds **1**, **2**, and **10** and by ECD calculations for compounds **5** and **6**. Compounds **3**−**6** showed potent cytotoxicity against the L5178Y murine lymphoma cell line with IC_{50} values of 0.7, 5.6, 3.4, and 3.9 μM, respectively. The presence of an epoxy group, the rearrangement of the double bond, and the methoxy substituent influenced their cytotoxicity differently, whereas the configuration of the C-8/C-9 double bond and the absolute configuration of C-4 had little influence with regard to the bioactivity of the respective metabolites. In addition, compound **5** exhibited significant activity against the human ovarian cancer cell line A2780 with an IC_{50} value of 1.2 μM. Moreover, when *P. microspora* was cocultured with *S. lividans*, the production of macrolides **5** and **6** strongly increased in comparison to the axenically grown fungus.

EXPERIMENTAL SECTION

General Experimental Procedures. Optical rotations were measured with a P-1020 polarimeter (JASCO). UV spectra were obtained from a PerkinElmer Lambda 25 UV/vis spectrometer. IR spectra were measured in ATR-mode (Platinum ATR-QL, Diamond) on a Bruker TENSOR 37 IR spectrometer. The melting point was determined using a Büchi melting point apparatus B-540. ^{1}H, ^{13}C, and 2D NMR spectra were recorded on Bruker Avance III 600 or 700 NMR spectrometers (Bruker). HRESIMS data were obtained from a UHR-QTOF Maxis 4G mass spectrometer (Bruker Daltonics). HPLC analysis was undertaken with a Dionex P580 system (Dionex Softron), employing a 125 × 4 mm i.d., 5 μm, Eurospher C_{18} analytical column (Knauer). Semipreparative HPLC was achieved on a Lachrom-Merck Hitachi system (Merck), using a 300 × 8 mm i.d., 10 μm, Eurospher C_{18} column (Knauer). Thin-layer chromatography was performed on precoated silica gel 60 F_{254} plates (Merck) with detection at 254 or 365 nm or by spraying anisaldehyde reagent followed by heating. Column chromatography was carried out using silica gel 60 M (Merck) or Sephadex LH-20.

Fungal Material and Identification. Following standard procedures,[17] the endophytic fungus was isolated from fresh, healthy fruits of *Drepanocarpus lunatus* (Fabaceae), which were collected in August 2013 from Douala, Cameroon. It was identified as *Pestalotiopsis microspora* (GenBank accession number KU255793) according to DNA amplification and sequencing of the fungal ITS region as described before.[18] A voucher fungal strain was kept in one of the authors' lab (P.P.) with the code number DL-F-3.

Fermentation, Extraction, and Isolation. Twenty 1 L Erlenmeyer flasks with solid rice medium (100 g of rice, 3.5 g of sea salt, and 110 mL of demineralized water, each) were used for fermentation. They were autoclaved at 121 °C for 20 min and cooled to room temperature, followed by inoculation with the fungus. After cultivation at 20 °C under static conditions for 4 weeks, 500 mL of EtOAc was added to each flask to stop the fermentation. The flasks were shaken at 150 rpm for 8 h on a shaker, and then the EtOAc solution was evaporated to dryness. The obtained brown extract (15.4 g) was subjected to a 20 × 8 cm i.d. silica gel vacuum liquid chromatography column, using solvents in a gradient of increasing

DOI: 10.1021/acs.jnatprod.6b00473
J. Nat. Prod. 2016, 79, 2332−2340

polarity (*n*-hexane−EtOAc, 9:1, 7:3, 1:1, 3:7; CH_2Cl_2−MeOH, 15:1, 9:1, 7:3, 0:10; 600 mL each gradient) to yield 11 fractions in total. Fractions C, E, and F, which showed bioactivity against the mouse lymphoma cell line, were selected for further separation. Fraction C (153.3 mg) was subjected to a 60 × 3 cm i.d. Sephadex LH-20 column with MeOH as mobile phase to remove pigments, then purified by semipreparative HPLC (MeOH−H_2O: 0−5 min, 45%; 5−15 min, from 45% to 58%; 16−19 min, 100%) to give **3** (2.1 mg), **4** (0.4 mg), and **8** (0.9 mg). Following the same protocol, a mixture (15.1 mg) of **1** and **9** was obtained from fraction E (149.8 mg) (HPLC sequence, MeOH−H_2O: 0−10 min, from 20% to 40%; 10−25 min, from 40% to 60%; 26−30 min, 100%). The mixture was subsequently separated by a Phenomenex chiral-phase column (250 × 4.6 mm i.d., 5 μm, Lux Amylose-2) using CH_3CN−H_2O (45:55), to afford **9** (9.3 mg) and **1** (3.2 mg). Meanwhile, **2** (5.4 mg), **5** (13.4 mg), **7** (3.4 mg), **6** (1.9 mg), and a mixture (51.2 mg) of **10** and **11** were obtained from fraction F (240.0 mg) (HPLC sequence, methanol−H_2O: 0−10 min, from 10% to 30%; 10−23 min, from 40% to 60%; 24−28 min, 100%). After separation by chiral-phase column as mentioned above, 10 mg of this mixture yielded **10** (4.5 mg) and **11** (4.5 mg).

*Pestalotioprolide B (**1**):* colorless crystals; mp 111−115 °C; $[\alpha]^{20}_D$ +72 (*c* 1.0, $CHCl_3$); UV (MeOH) λ_{max} (log ε) 214 (3.55) nm; IR ν_{max} 3373, 2939, 1714, 1687, 1368, 1241, 1043, 971 cm^{-1}; ^1H and ^{13}C NMR data, Table 1; HRESIMS *m*/*z* 291.1207 $[M + Na]^+$ (calcd for $C_{14}H_{20}NaO_5$, 291.1203).

*Pestalotioprolide C (**2**):* colorless crystals; mp 124−126 °C; $[\alpha]^{20}_D$ +40 (*c* 1.4, MeOH); UV (MeOH) λ_{max} (log ε) 218 (3.66) nm; IR ν_{max} 3294, 2933, 1704, 1644, 1483, 1265, 1127, 1058, 966 cm^{-1}; ^1H and ^{13}C NMR data, Table 1; HRESIMS *m*/*z* 257.1748 $[M + H]^+$ (calcd for $C_{14}H_{25}O_4$, 257.1747).

*7-O-Methylnigrosporolide (**3**):* colorless oil; $[\alpha]^{20}_D$ +67 (*c* 0.2, MeOH); UV (MeOH) λ_{max} (log ε) 214 (3.54) nm; IR ν_{max} 3298, 2934, 1704, 1645, 1482, 1352, 1264, 1127, 1058, 1027 cm^{-1}; ^1H and ^{13}C NMR data, Table 1; HRESIMS *m*/*z* 289.1407 $[M + Na]^+$ (calcd for $C_{15}H_{22}NaO_4$, 289.1410).

*Pestalotioprolide D (**4**):* colorless oil; $[\alpha]^{20}_D$ −30 (*c* 0.1, MeOH); UV (MeOH) λ_{max} (log ε) 220 (3.45) nm; IR ν_{max} 3300, 2935, 1705, 1645, 1483, 1266, 1108, 1059, 966 cm^{-1}; ^1H and ^{13}C NMR data, Table 1; HRESIMS *m*/*z* 289.1408 $[M + Na]^+$ (calcd for $C_{15}H_{22}NaO_4$, 289.1410).

*Pestalotioprolide E (**5**):* colorless oil; $[\alpha]^{20}_D$ +222 (*c* 1.8, MeOH); ECD (MeCN) λ_{max} ($\Delta\varepsilon$) 295 (sh) (+0.86), 234 (+22.97), negative CE below 202 nm; UV (MeOH) λ_{max} (log ε) 214 (4.25), 230 (4.15) nm; IR ν_{max} 3379, 2939, 1696, 1642, 1453, 1265, 1081, 989 cm^{-1}; ^1H and ^{13}C NMR data, Table 2; HRESIMS *m*/*z* 270.1698 $[M + NH_4]^+$ (calcd for $C_{14}H_{24}NO_4$, 270.1700).

*Pestalotioprolide F (**6**):* colorless oil; $[\alpha]^{20}_D$ +9 (*c* 0.5, MeOH); ECD (MeCN) λ_{max} ($\Delta\varepsilon$) 351 (+0.09), 288 (−0.07), 233 (+1.31), 207 (−1.83) nm; UV (MeOH) λ_{max} (log ε) 211 (4.24), 229 (4.14) nm; IR ν_{max} 3380, 2934, 1703, 1650, 1451, 1259, 1108, 979 cm^{-1}; ^1H and ^{13}C NMR data, Table 2; HRESIMS *m*/*z* 270.1701 $[M + NH_4]^+$ (calcd for $C_{14}H_{24}NO_4$, 270.1700).

*Pestalotioprolide G (**7**):* colorless oil; $[\alpha]^{20}_D$ −177 (*c* 0.2, MeOH); UV (MeOH) λ_{max} (log ε) 265 (4.33) nm; IR ν_{max} 3420, 2938, 1714, 1584, 1451, 1360, 1254, 1110, 976 cm^{-1}; ^1H and ^{13}C NMR data, Table 2; HRESIMS *m*/*z* 253.1436 $[M + H]^+$ (calcd for $C_{14}H_{21}O_4$, 253.1434).

*Pestalotioprolide H (**8**):* colorless oil; $[\alpha]^{20}_D$ −38 (*c* 0.2, MeOH); UV (MeOH) λ_{max} (log ε) 264 (4.34) nm; ^1H and ^{13}C NMR data, Table 2; HRESIMS *m*/*z* 267.1586 $[M + H]^+$ (calcd for $C_{15}H_{23}O_4$, 267.1591).

*Seiricuprolide (**9**):* white powder; $[\alpha]^{20}_D$ +40 (*c* 2.7, MeOH), lit.[3] $[\alpha]^{25}_D$ +67 (*c* 1.5, MeOH).

*Nigrosporolide (**10**):* colorless crystals; mp 142−145 °C; $[\alpha]^{20}_D$ +81 (*c* 0.9, MeOH).

*4,7-Dihydroxy-13-tetradeca-2,5,8-trienolide (**11**):* white powder; $[\alpha]^{20}_D$ +174 (*c* 0.4, $CHCl_3$), lit.[15] $[\alpha]^{28}_D$ +188 (*c* 0.7, $CHCl_3$).

X-ray Crystallographic Analysis of 1, 2, and 10. *Crystallization Conditions.* X-ray quality crystals of **1**, **2**, and **10** were obtained by slow evaporation from an acetone solution. A suitable single crystal was carefully selected under a polarizing microscope. Data collection: Bruker Kappa APEX2 CCD diffractometer with a microfocus tube, Cu Kα radiation (λ = 1.541 78 Å) for **1**, **2**, and the first data set of **10** or Mo Kα radiation (λ = 0.710 73 Å) for the second data set of **10**, multilayer mirror, ω- and ϕ-scan; data collection with APEX2, cell refinement and data reduction with SAINT,[19] experimental absorption correction with SADABS.[20] Structure analysis and refinement: The structure was solved by direct methods using SHELXS-97; refinement was done by full-matrix least-squares on F^2 using the SHELXL-97 program suite.[21] All non-hydrogen positions were refined with anisotropic displacement parameters. Hydrogen atoms were positioned geometrically (with C−H = 0.95 Å for aromatic CH, 1.00 Å for tertiary CH, 0.99 Å for CH_2, and 0.98 Å for CH_3) and refined using riding models (AFIX 43, 13, 23, and 137, respectively), with $U_{iso}(H) = 1.2U_{eq}(CH, CH_2)$ and $1.5U_{eq}(CH_3)$. The hydrogen atoms in the hydroxy groups were positioned geometrically with AFIX 148 in **1** and were found and refined with $U_{iso}(H) = 1.5U_{eq}(O)$ in **2** and **10**. Hydrogen atoms in the solvent water molecule in **1** were found and refined with $U_{iso}(H) = 1.5U_{eq}(O)$.

During refinement of the data set for compound **2**, SHELX reported warnings regarding the Flack parameter. The Flack parameter calculated by classical fit to all intensities gave a value of −0.0(9), and the Flack parameter calculated by Parsons' method gave 0.25(15) together with the message "Friedel differences statistically dubious - Flack x unreliable". The refinement as a two-component inversion twin using the TWIN/BASF instructions in SHELXL led to a Flack parameter of 0.00, a negative BASF, and continuing errors. Therefore, the analysis of the absolute configuration was performed using likelihood methods[22] with the command "BywoetPair" in PLATON for Windows.[23] The resulting value for the Hooft parameter was given as 0.17(12), which indicated that the absolute configuration was probably determined correctly. The method calculated the probability that the absolute configuration of the model was correct as 1.00 P2(true).[22]

For compound **10** the Mo Kα data set was collected for the bond length and angle information, while the Cu Kα data set was crucial for the absolute configuration.

Graphics were drawn with DIAMOND,[24] and analyses of the inter- and intramolecular hydrogen-bonding interactions were done with PLATON for Windows.[23] The structural data have been deposited in the Cambridge Crystallographic Data Center (CCDC Nos. 1479850 for **1**, 1479851 for **2**, 1479852 and 1479853 for **10**).

*Crystal data of **1**:* $C_{14}H_{22}O_6$, *M* = 286.31, triclinic system, space group *P*1, *a* = 6.3082(4) Å, *b* = 7.5108(5) Å, *c* = 8.1100(5) Å, *V* = 374.29(4) Å^3, *Z* = 1, D_{calc} = 1.270 g/cm^3, crystal size 0.11 × 0.09 × 0.05 mm^3, μ(Cu Kα) = 0.827 mm^{-1}, 5.5° < θ < 65.3°, N_t = 3068, *N* = 1630 (R_{int} = 0.0449), R_1 = 0.0342, wR_2 = 0.0878, *S* = 1.026, Flack parameter[25] = −0.03(19).

*Crystal data of **2**:* $C_{14}H_{24}O_4$, *M* = 256.33, orthorhombic system, space group $P2_12_12_1$, *a* = 36.533(4) Å, *b* = 4.9693(6) Å, *c* = 7.6479(9) Å, *V* = 1388.4(3) Å^3, *Z* = 4, D_{calc} = 1.226 g/cm^3, crystal size 0.30 × 0.08 × 0.04 mm^3, μ(Cu Kα) = 0.717 mm^{-1}, 2.4° < θ < 71.9°, N_t = 17343, *N* = 2418 (R_{int} = 0.0668), R_1 = 0.0867, wR_2 = 0.2408, *S* = 1.161, Hooft parameter = 0.17(12).

*Crystal data of **10** (Cu Kα):* $C_{14}H_{20}O_4$, *M* = 252.30, orthorhombic system, space group $P2_12_12_1$, *a* = 4.8106(3) Å, *b* = 7.6079(5) Å, *c* = 37.246(2) Å, *V* = 1363.13(15) Å^3, *Z* = 4, D_{calc} = 1.229 g/cm^3, crystal size 0.80 × 0.10 × 0.02 mm^3, μ(Cu Kα) = 0.730 mm^{-1}, 2.4° < θ < 44.5°, N_t = 4063, *N* = 928 (R_{int} = 0.0541), R_1 = 0.0287, wR_2 = 0.0687, *S* = 1.159, Flack parameter = 0.14(8).

*Crystal data of **10** (Mo Kα):* $C_{14}H_{20}O_4$, *M* = 252.30, orthorhombic system, space group $P2_12_12_1$, *a* = 4.8042(3) Å, *b* = 7.6036(4) Å, *c* = 37.247(2) Å, *V* = 1360.59(13) Å^3, *Z* = 4, D_{calc} = 1.232 g/cm^3, crystal size 0.80 × 0.10 × 0.02 mm^3, μ(Mo Kα) = 0.089 mm^{-1}, 2.2° < θ < 26.5°, N_t = 21569, *N* = 2786 (R_{int} = 0.0294), R_1 = 0.0316, wR_2 = 0.0797, *S* = 1.088.

Preparation of (*S*)- and (*R*)-MTPA Esters 5a and 5b. Compound **5** (0.8 mg) was treated with (*R*)-MTPACl (8 μL) and DMAP (0.1 mg) in 0.5 mL of pyridine. The mixture was stirred at room temperature for 12 h. The crude product was purified by semipreparative HPLC (MeOH−H_2O: 0−5 min, 60%; 5−15 min,

DOI: 10.1021/acs.jnatprod.6b00473
J. Nat. Prod. 2016, 79, 2332−2340

from 60% to 90%; 16−19 min, 100%), to yield (*S*)-MTPA ester **5a** (1.6 mg). In a similar way, (*R*)-MTPA ester **5b** (1.6 mg) was prepared after compound **5** reacted with (*S*)-MTPACl.

*(S)-MTPA ester **5a**:* ^{1}H NMR (CD_3OD, 600 MHz) δ 7.62−7.41 (10H, m, phenyl protons), 6.70 (1H, dd, J = 15.8, 10.1 Hz, H-7), 6.40 (1H, dd, J = 10.7, 10.1 Hz, H-6), 5.90 (1H, d, J = 10.7 Hz, H-5), 5.72 (1H, dd, J = 15.8, 5.3 Hz, H-8), 5.69 (1H, m, H-9), 5.49 (1H, dd, J = 10.1, 5.7 Hz, H-3), 5.03 (1H, m, H-13), 3.63 (3H, s, OMe of MTPA), 3.55 (3H, s, OMe of MTPA), 2.99 (1H, dd, J = 15.1, 5.7 Hz, H-2a), 2.90 (1H, dd, J = 15.1, 10.1 Hz, H-2b), 1.92 (1H, m, H-10a), 1.82 (1H, m, H-10b), 1.76 (1H, m, H-12a), 1.64 (1H, m, H-12b), 1.57 (2H, m, H_2-11), 1.24 (3H, d, J = 6.4 Hz, H_3-14); HRESIMS m/z 702.2501 $[M + NH_4]^+$ (calcd for $C_{34}H_{38}F_6NO_8$, 702.2496).

*(R)-MTPA ester **5b**:* ^{1}H NMR (CD_3OD, 600 MHz) δ 7.58−7.43 (10H, m, phenyl protons), 6.75 (1H, dd, J = 16.2, 10.2 Hz, H-7), 6.45 (1H, dd, J = 10.7, 10.2 Hz, H-6), 5.87 (1H, dd, J = 16.2, 5.1 Hz, H-8), 5.86 (1H, d, J = 10.7 Hz, H-5), 5.71 (1H, m, H-9), 5.50 (1H, dd, J = 9.8, 6.1 Hz, H-3), 4.99 (1H, m, H-13), 3.61 (3H, s, OMe of MTPA), 3.57 (3H, s, OMe of MTPA), 3.04 (1H, dd, J = 15.0, 6.1 Hz, H-2a), 2.97 (1H, dd, J = 15.0, 9.8 Hz, H-2b), 1.82 (1H, m, H-10a), 1.73 (1H, m, H-10b), 1.66 (1H, m, H-12a), 1.56 (1H, m, H-12b), 1.51 (1H, m, H-11a), 1.38 (1H, m, H-11b), 1.21 (3H, d, J = 6.3 Hz, H_3-14); HRESIMS m/z 702.2496 $[M + NH_4]^+$ (calcd for $C_{34}H_{38}F_6NO_8$, 702.2496).

Cocultivation Experiment of *P. microspora* with *S. lividans*. *P. microspora* and *S. lividans* were cocultured in 15 1-L Erlenmeyer flasks (three for axenic *P. microspora*, three for axenic *S. lividans*, three for coculture of *P. microspora* and 0.05 g of *S. lividans*, three for coculture of *P. microspora* and 0.1 g of *S. lividans*, three for coculture of *P. microspora* and 0.2 g of *S. lividans*) containing 60 mL of yeast malt (YM) medium and 50 g of commercially available rice each. An overnight culture of *S. lividans* was inoculated to prewarmed YM medium, which was then incubated at 37 °C and shaken at 200 rpm for 15 h. The resulting *S. lividans* balls were separated from the broth after centrifugation at 6000 rpm for 5 min. After weighing, 1.4 g of *S. lividans* balls was suspended with 7 mL of fresh YM medium and then added to the coculture flasks (0.05, 0.1, or 0.2 g/flask), which were further incubated at 30 °C for 7 days. After this preincubation, *P. microspora* grown on malt agar was added under sterile conditions. Then all flasks were kept at 20 °C under static conditions until they reached the stationary growth phase (3 weeks for control of *P. microspora* and *S. lividans*, 5 weeks for coculture). The fermentation was stopped by adding 500 mL of EtOAc to each flask. After evaporation, the dry extract was dissolved in 20 mL of MeOH, and 25 μL of this solution was injected for HPLC analysis.

Cytotoxicity Assay. Cytotoxicity against the mouse lymphoma cell line L5178Y and the human ovarian cancer cell line A2780 was evaluated using the MTT method with kahalalide F (for L5178Y) or cisplatin (for A2780) as positive control and media with 0.1% DMSO as negative control as described previously.[26,27]

Computational Section. Mixed torsional/low-frequency mode conformational searches were carried out by means of the Macromodel 9.9.223 software using the Merck Molecular Force Field (MMFF) with an implicit solvent model for $CHCl_3$.[28] Geometry reoptimizations were carried out at the B3LYP/6-31G(d) level in vacuo and at the B97D/TZVP[29,30] and CAM-B3LYP/TZVP[31,32] levels with the PCM solvent model for MeCN. TDDFT-ECD calculations were run with various functionals (B3LYP, BH&HLYP, CAM-B3LYP, PBE0) and the TZVP basis set as implemented in the Gaussian 09 package with the same or no solvent model as in the preceding DFT optimization step.[33] ECD spectra were generated as sums of Gaussians with 3000 and 4200 cm^{-1} widths at half-height (corresponding to ca. 16 and 22 at 230 nm, respectively), using dipole-velocity-computed rotational strength values.[34] Boltzmann distributions were estimated from the ZPVE-corrected B3LYP/6-31G(d) energies in the gas-phase calculations and from the B97D/TZVP and CAM-B3LYP/TZVP energies in the solvated ones. The MOLEKEL software package was used for visualization of the results.[35]

■ ASSOCIATED CONTENT

Supporting Information

The Supporting Information is available free of charge on the ACS Publications website at DOI: 10.1021/acs.jnatprod.6b00473.

UV, HRESIMS, and NMR spectra of compounds **1**−**8** and MTPA esters **5a** and **5b**, and structure and population of the low-energy conformers (>1%) of compounds **5** and **6** as well as results of X-ray analysis of compounds **1**, **2**, and **10** (PDF)

Crystallographic data (CIF)

Crystallographic data (CIF)

Crystallographic data (CIF)

■ AUTHOR INFORMATION

Corresponding Authors

*Tel: +49 211 81 15979. Fax: +49 211 81 11923. E-mail: zhenfeizi0@sina.com (Z. Liu).

*Tel: +49 211 81 14163. Fax: +49 211 81 11923. E-mail: proksch@uni-duesseldorf.de (P. Proksch).

Notes

The authors declare no competing financial interest.

■ ACKNOWLEDGMENTS

S.L. thanks the China Scholarship Council for financial support. P.P. wishes to thank the Manchot Foundation and the DFG (GRK 2158) for support. T.K. and A.M. thank the Hungarian National Research Foundation (OTKA K105871) for financial support and the National Information Infrastructure Development Institute (NIIFI 10038) for CPU time. We furthermore wish to thank S. H. Akone (Institute of Pharmaceutical Biology and Biotechnology, Heinrich-Heine-Universität Düsseldorf, Germany) for collection of the plant material.

■ REFERENCES

(1) McGuire, J. M.; Bunch, R. L.; Anderson, R. C.; Boaz, H. E.; Flynn, E. H.; Powell, H. M.; Smith, J. W. *Antibiot. Chemother.* **1952**, *2*, 281−283.

(2) Harvey, R. J.; Wallwork, B. D.; Lund, V. J. *Immunol. Allergy Clin. North Am.* **2009**, *29*, 689−703.

(3) Ballio, A.; Evidente, A.; Graniti, A.; Randazzo, G.; Sparapano, L. *Phytochemistry* **1988**, *27*, 3117−3121.

(4) Zinedine, A.; Soriano, J. M.; Moltó, J. C.; Mañes, J. *Food Chem. Toxicol.* **2007**, *45*, 1−18.

(5) Kito, K.; Ookura, R.; Yoshida, S.; Namikoshi, M.; Ooi, T.; Kusumi, T. *Org. Lett.* **2008**, *10*, 225−228.

(6) Xu, J.; Kjer, J.; Sendker, J.; Wray, V.; Guan, H.; Edrada, R.; Lin, W.; Wu, J.; Proksch, P. *J. Nat. Prod.* **2009**, *72*, 662−665.

(7) Bara, R.; Zerfass, I.; Aly, A. H.; Goldbach-Gecke, H.; Raghavan, V.; Sass, P.; Mándi, A.; Wray, V.; Polavarapu, P. L.; Pretsch, A.; Lin, W.; Kurtán, T.; Debbab, A.; Brötz-Oesterhelt, H.; Proksch, P. *J. Med. Chem.* **2013**, *56*, 3257−3272.

(8) El Amrani, M.; Lai, D.; Debbab, A.; Aly, A. H.; Siems, K.; Seidel, C.; Schnekenburger, M.; Gaigneaux, A.; Diederich, M.; Feger, D.; Lin, W.; Proksch, P. *J. Nat. Prod.* **2014**, *77*, 49−56.

(9) Liu, S.; Dai, H.; Orfali, R. S.; Lin, W.; Liu, Z.; Proksch, P. *J. Agric. Food Chem.* **2016**, *64*, 3127−3132.

(10) Ola, A. R. B.; Thomy, D.; Lai, D.; Brötz-Oesterhelt, H.; Proksch, P. *J. Nat. Prod.* **2013**, *76*, 2094−2099.

(11) Chen, H.; Daletos, G.; Abdel-Aziz, M. S.; Thomy, D.; Dai, H.; Brötz-Oesterhelt, H.; Lin, W.; Proksch, P. *Phytochem. Lett.* **2015**, *12*, 35−41.

(12) Rukachaisirikul, V.; Rodglin, A.; Phongpaichit, S.; Buatong, J.; Sakayaroj, J. *Phytochem. Lett.* **2012**, *5*, 13−17.

DOI: 10.1021/acs.jnatprod.6b00473
J. Nat. Prod. 2016, 79, 2332−2340

(13) Harwooda, J. S.; Cutler, H. G.; Jacyno, J. M. *Nat. Prod. Lett.* **1995**, *6*, 181−185.
(14) Jiao, P.; Swenson, D. C.; Gloer, J. B.; Wicklow, D. T. *J. Nat. Prod.* **2006**, *69*, 636−639.
(15) Kobayashi, H.; Kanematsu, M.; Yoshida, M.; Shishido, K. *Chem. Commun.* **2011**, *47*, 7440−7442.
(16) Khamthong, N.; Rukachaisirikul, V.; Phongpaichit, S.; Preedanon, S.; Sakayroj, J. *Phytochem. Lett.* **2014**, *10*, 5−9.
(17) Debbab, A.; Aly, A. H.; Edrada-Ebel, R.; Wray, V.; Müller, W. E. G.; Totzke, F.; Zirrgiebel, U.; Schächtele, C.; Kubbutat, M. H. G.; Lin, W. H.; Mosaddak, M.; Hakiki, A.; Proksch, P.; Ebel, R. *J. Nat. Prod.* **2009**, *72*, 626−631.
(18) Kjer, J.; Debbab, A.; Aly, A. H.; Proksch, P. *Nat. Protoc.* **2010**, *5*, 479−490.
(19) *Apex2, Data Collection Program for the CCD Area-Detector System*; *SAINT, Data Reduction and Frame Integration Program for the CCD Area-Detector System*; Bruker Analytical X-ray Systems: Madison, WI, USA, 1997−2006.
(20) Sheldrick, G. M. *SADABS: Area-detector absorption correction*; University of Göttingen: Germany, 1996.
(21) Sheldrick, G. M. *Acta Crystallogr., Sect. A: Found. Crystallogr.* **2008**, *64*, 112−122.
(22) (a) Hooft, R. W. W.; Straver, L. H.; Spek, A. L. *J. Appl. Crystallogr.* **2008**, *41*, 96−103. (b) Hooft, R. W. W.; Straver, L. H.; Spek, A. L. *Acta Crystallogr., Sect. A: Found. Crystallogr.* **2009**, *65*, 319−321. (c) Hooft, R. W. W.; Straver, L. H.; Spek, A. L. *J. Appl. Crystallogr.* **2010**, *43*, 665−668.
(23) (a) Spek, A. L. *Acta Crystallogr., Sect. D: Biol. Crystallogr.* **2009**, *65*, 148−155. (b) Spek, A. L. *J. Appl. Crystallogr.* **2003**, *36*, 7−13. (c) Spek, A. L. *PLATON - A Multipurpose Crystallographic Tool*; Utrecht University: Utrecht, The Netherlands, 2008. (d) Farrugia, L. J. *Windows implementation*, Version 40608; University of Glasgow: Scotland, 2008.
(24) Brandenburg, K. *Diamond (Version 3.2), Crystal and Molecular Structure Visualization, Crystal Impact − K*; Brandenburg & H. Putz Gbr: Bonn, Germany, 2009.
(25) (a) Flack, H. D.; Sadki, M.; Thompson, A. L.; Watkin, D. J. *Acta Crystallogr., Sect. A: Found. Crystallogr.* **2011**, *67*, 21−34. (b) Flack, H. D.; Bernardinelli, G. *Chirality* **2008**, *20*, 681−690. (c) Flack, H. D.; Bernardinelli, G. *Acta Crystallogr., Sect. A: Found. Crystallogr.* **1999**, *55*, 908−915. (d) Flack, H. *Acta Crystallogr., Sect. A: Found. Crystallogr.* **1983**, *39*, 876−881.
(26) Ashour, M.; Edrada, R.; Ebel, R.; Wray, V.; Wätjen, W.; Padmakumar, K.; Müller, W. E. G.; Lin, W. H.; Proksch, P. *J. Nat. Prod.* **2006**, *69*, 1547−1553.
(27) Rönsberg, D.; Debbab, A.; Mandi, A.; Vasylyeva, V.; Böhler, P.; Stork, B.; Engelke, L.; Hamacher, A.; Sawadogo, R.; Diederich, M.; Wray, V.; Lin, W.; Kassack, M. U.; Janiak, C.; Scheu, S.; Wesselborg, S.; Kurtan, T.; Aly, A. H.; Proksch, P. *J. Org. Chem.* **2013**, *78*, 12409−12425.
(28) *MacroModel*; Schrödinger, LLC, 2012, http://www.schrodinger.com/MacroModel.
(29) Sun, P.; Xu, D. X.; Mándi, A.; Kurtán, T.; Li, T. J.; Schulz, B.; Zhang, W. *J. Org. Chem.* **2013**, *78*, 7030−7047.
(30) Grimme, S. *J. Comput. Chem.* **2006**, *27*, 1787−1799.
(31) Yanai, T.; Tew, D.; Handy, N. *Chem. Phys. Lett.* **2004**, *393*, 51−57.
(32) Pescitelli, G.; Di Bari, L.; Berova, N. *Chem. Soc. Rev.* **2011**, *40*, 4603−4625.
(33) Frisch, M. J.; Trucks, G. W.; Schlegel, H. B.; Scuseria, G. E.; Robb, M. A.; Cheeseman, J. R.; Scalmani, G.; Barone, V.; Mennucci, B.; Petersson, G. A.; Nakatsuji, H.; Caricato, M.; Li, X.; Hratchian, H. P.; Izmaylov, A. F.; Bloino, J.; Zheng, G.; Sonnenberg, J. L.; Hada, M.; Ehara, M.; Toyota, K.; Fukuda, R.; Hasegawa, J.; Ishida, M.; Nakajima, T.; Honda, Y.; Kitao, O.; Nakai, H.; Vreven, T.; Montgomery, J. A., Jr.; Peralta, J. E.; Ogliaro, F.; Bearpark, M.; Heyd, J. J.; Brothers, E.; Kudin, K. N.; Staroverov, V. N.; Kobayashi, R.; Normand, J.; Raghavachari, K.; Rendell, A.; Burant, J. C.; Iyengar, S. S.; Tomasi, J.; Cossi, M.; Rega, N.; Millam, J. M.; Klene, M.; Knox, J. E.; Cross, J. B.; Bakken, V.; Adamo, C.; Jaramillo, J.; Gomperts, R.; Stratmann, R. E.; Yazyev, O.; Austin, A. J.; Cammi, R.; Pomelli, C.; Ochterski, J. W.; Martin, R. L.; Morokuma, K.; Zakrzewski, V. G.; Voth, G. A.; Salvador, P.; Dannenberg, J. J.; Dapprich, S.; Daniels, A. D.; Farkas, O.; Foresman, J. B.; Ortiz, J. V.; Cioslowski, J.; Fox, D. J. *Gaussian 09*, revision B.01; Gaussian, Inc.: Wallingford, CT, 2010.
(34) Stephens, P. J.; Harada, N. *Chirality* **2010**, *22*, 229−233.
(35) Varetto, U. *MOLEKEL*, v. 5.4; Swiss National Supercomputing Centre: Manno, Switzerland, 2009.

DOI: 10.1021/acs.jnatprod.6b00473
J. Nat. Prod. 2016, 79, 2332−2340